NeuroImage 181 (2018) 748–759

Contents lists available at ScienceDirect

NeuroImage

journal homepage: www.elsevier.com/locate/neuroimage

Columnar organization of mid-spectral and end-spectral hue preferences in human visual cortex

Shahin Nasr [a,b,*], Roger B.H. Tootell [a,b]

[a] Athinoula A. Martinos Center for Biomedical Imaging, Massachusetts General Hospital, Boston, MA, USA
[b] Department of Radiology, Harvard Medical School, Boston, MA, USA

A B S T R A C T

Multiple color-selective areas have been described in visual cortex, in both humans and non-human primates. In macaques, hue-selective columns have been reported in several areas. In V2, it has been proposed that such hue-selective columns are mapped so as to mirror the order of wavelength through the visible spectrum, within thin-type stripes. Other studies have suggested a neural segregation of mid-spectral vs. end-spectral hue preferences (e.g. red and blue vs. green and yellow), within thin- and thick-type stripes, respectively. This latter segregation could reduce the spatial 'blur' due to chromatic aberration in the encoding of fine spatial details in the thick-type stripes.

To distinguish between these and related models, we tested the organization of hue preferences in human visual cortex using fMRI at high spatial resolution. We used a high field (7T) scanner in humans (n = 7), measuring responses to four independent hues, including end-spectral (i.e. red-gray and blue-gray) and mid-spectral (i.e. green-gray and yellow-gray) isoluminant gratings, and also relative to achromatic luminance-varying (control) stimuli. In each subject, thin- and thick-type columns in V2 and V3 were localized using an independent set of stimuli and scans.

We found distinct hue-selective differences along the dimension of mid-vs. end-spectral hues, in striate and early extrastriate visual cortex. First, as reported previously in macaques, V1 responded more strongly to end-spectral hues, compared to mid-spectral hues. Second, the color-selective thin-type stripes in V2 and V3 showed a greater response to end- and mid-spectral hues, relative to luminance-varying gratings. Third, thick-type stripes in V2/V3 showed a significantly stronger response to mid-spectral (compared to end-spectral) hues. Fourth, in the higher-tier color-selective area in occipital temporal cortex (n = 4), responses to all four hues were statistically equivalent to each other.

These results suggest that early visual cortex segregates the processing of mid-vs. end-spectral hues, perhaps to counter the challenging optical constraint of chromatic aberration.

1. Introduction

Humans can see a narrow range of wavelengths within the electromagnetic spectrum, roughly from 400 – 700 nm. Nevertheless within that range, typical human observers can discriminate many different variations in light (Geldard, 1972; Judd and Wyszecki, 1975). Such variations can be grouped into three main perceptual dimensions: hue, saturation and luminance, which are related to physical variations of wavelength, spectral purity, and intensity, respectively. Here we focus on sensitivity to variations in hue/wavelength.

In humans (Zeki et al., 1991; Hadjikhani et al., 1998; Beauchamp et al., 1999; Bartels and Zeki, 2000; Mullen et al., 2007; Lafer-Sousa et al., 2016; Nasr et al., 2016) and other primates (Zeki, 1983; Livingstone and Hubel, 1984; Tootell et al., 2004; Lu and Roe, 2008; Wade et al., 2008; Lim et al., 2009), multiple studies have reported neural clusters or areas that respond selectively to hue-varying (rather than luminance-varying) stimuli, in different visual areas, including striate and extrastriate cortex.

At a smaller spatial scale, Zeki was first to report hue-selective 'color columns' in a fourth-named area (V4) in macaque visual cortex (Zeki, 1973, 1983). In such columns, neurons that respond selectively to a given stimulus hue (e.g. either red, green, or blue) are grouped together along a radial (vertical) axis, i.e. perpendicular to the cortical surface.

Given such hue-selective columns, one might ask how columns for different hues are mapped across the cortical surface. One model proposes a spatially continuous 1D arrangement of preferred hues that mirrors the continuous variation in wavelength through the visible spectrum (Xiao et al., 2003; Lim et al., 2009; Tanigawa et al., 2010). For instance, a cortical column that responds selectively to blue (i.e. dominated by short wavelengths) would be located adjacent to cortical sites that preferred green, then yellow, then red, (i.e. progressively longer wavelengths), or vice versa. For convenience, we describe this as a 'spectral' model of hue mapping. Such an organization was reported in V1 (Ts'o and Gilbert, 1988, Roe and Ts'o, 1999, Landisman and Ts' O, 2002a, b, Xiao et al., 2007, Xiao et al., 2011), and in detail in V2, as a

* Corresponding author. Athinoula A. Martinos Center for Biomedical Imaging, Massachusetts General Hospital, Boston, MA, USA.
E-mail address: shahin@nmr.mgh.harvard.edu (S. Nasr).

https://doi.org/10.1016/j.neuroimage.2018.07.053
Received 20 January 2018; Received in revised form 21 June 2018; Accepted 23 July 2018
Available online 25 July 2018

subdivision of larger color-selective stripes in this area (Xiao et al., 2003, Lim et al., 2009).A similar spectral organization of hue selectivity was also reported within color-selective patches of area V4 (Tanigawa et al., 2010) and higher level visual areas (Chang et al., 2017).

An alternative hypothesis of hue mapping was proposed by Dow et al. (Vautin and Dow, 1985; Yoshioka and Dow, 1996; Yoshioka et al., 1996; Dow, 2002), based on well-known optical constraints due to chromatic aberration (Walls, 1943; Hartridge, 1947). Briefly, in the linear form of chromatic aberration, wavelength-varying stimuli have different focal lengths on the retina, and without very specialized optical compensations (not present in the human eye), it is physically impossible to focus red and blue (i.e. end-spectral) stimuli on the retina at the same time. This results in blurring of the end-spectral stimuli on the retina, compared to the mid-spectral ones.

To reduce this problem, the Dow et al. model subdivides neural responses into those that are selective to mid-spectral hues (e.g. yellow and green), vs. those that are selective for end-spectral hues (e.g. blue and red). Only mid-spectral hues (for instance, green (~535 nm) and yellow (~575 nm)) are sampled in the processing of spatially-fine visual details, because such mid-spectral hues are subject to much reduced chromatic aberration. Comparison of information from a much wider range of hues (e.g. blue (470 nm) through red (630 nm) (i.e. a roughly four-fold greater difference compared to the mid-spectral range)) would be subject to much greater chromatic aberration. This may be partly why color processing has a reduced sensitivity to higher spatial frequencies, relative to luminance processing (Mullen, 1985; Webster et al., 1990; Anderson et al., 1991; Vimal, 2002).

This dichotomous end-vs. mid-spectral model has been supported by single unit recording in area V2 (Yoshioka and Dow, 1996; Yoshioka et al., 1996), in which segregated pathways are well-known based on histological (cytochrome oxidase) staining (Hubel and Livingstone, 1987; Tootell and Hamilton, 1989; Peterhans and von der Heydt, 1993; Vanduffel et al., 2002; Kaskan et al., 2009; Felleman et al., 2015). Specifically, a significant response was reported to mid-spectral hues within the thick-type (but not thin-type) stripes in macaque V2 (Yoshioka and Dow, 1996). In this and many additional studies, it has been reported that these thick-type stripes also selectively process fine-scale shape details, including orientation (Hubel and Livingstone, 1987; Yoshioka and Dow, 1996; Vanduffel et al., 2002; Kaskan et al., 2009). However, well-known sampling limitations of single unit recording, and differences in color vision between monkeys and humans (Dobkins et al., 2000), suggest that further study in humans would be informative.

More empirically, a third type of map-based variation in hue sensitivity has also been reported numerous times in monkey visual cortex, although it has not yet been clearly linked to any specific model of color processing. Specifically, studies in monkey V1 based on single units (Vautin and Dow, 1985; Creutzfeldt et al., 1987; Yoshioka et al., 1996), optical recording (Salzmann et al., 2012), and deoxyglucose mapping (Tootell et al., 1988) have all reported a robust response to end-spectral stimuli (e.g. red and blue), and a reduced response to mid-spectral hues (e.g. yellow and green). Again, this finding strongly suggests a segregated processing of mid-vs. end-spectral hues, even in striate cortex. However, it remains unknown whether such an end-spectral hue bias is present in humans as well as monkeys, and if confirmed, whether such a finding can be linked to the organization of hue described above. Here we addressed these questions, in the course of our main column-scale experiments on hue-selective cortical organization.

Despite the numerous studies that focused on localizing color-selective regions within human visual cortex, to the best of our knowledge, evidence for hue maps *per se* has not been reported. Some studies were simply not designed to test for hue mapping *per se*. For instance, several groups conducted elegant studies testing for variations in color sensitivity based on S-cone and L/M-cone stimuli (Engel et al., 1997; Liu and Wandell, 2005; Mullen et al., 2007; Sumner et al., 2008) using fMRI in visual cortex. However, in order to optimally activate cone-selective responses in these studies, it was necessary for such studies to present hue *pairs* – so that sensitivity to a given single hue could not be extracted from such data.

Another reason for the dearth of hue-selective maps in human visual cortex may be that such maps were simply too small to see based on conventional fMRI techniques based on the expected size of those neural columns that are involved in coding color (e.g. in V2 thin-type stripes) and related variables (e.g. in V2 thick-type stripes) in non-human primates. However, recent technical advances have made it possible to directly localize and study such functional columns in humans based on high-resolution fMRI (Yacoub et al., 2007, 2008; Zimmermann et al., 2011; Nasr et al., 2016; Dumoulin et al., 2017; Tootell and Nasr, 2017).

To test these models of hue processing in human visual cortex, we collected high-resolution fMRI activity evoked by each of four different hues in 7 human subjects using a 7T scanner. At the spatial scale of areas, we found a stronger response to end-spectral compared to mid-spectral hues in V1, as suggested by previous studies in non-human primates (Vautin and Dow, 1985; Creutzfeldt et al., 1987; Tootell et al., 1988; Salzmann et al., 2012). At the finer scale of cortical columns, and consistent with the model suggested by Dow et al., we found a strong bias for mid-spectral (compared to end-spectral) hues beyond color-selective thin-type columns in V2/V3, e.g. in thick-type stripes. In comparison, responses to all four hues were roughly equivalent to each other in the thin-type columns in V2 and V3, and in the color-selective area in occipital temporal cortex.

2. Methods

2.1. Participants

Seven human subjects (3 females and 4 males), aged 22–35 years, participated in this study. All subjects had normal color vision (based on Ishihara and Farnsworth D15 tests), normal or corrected-to-normal visual acuity, and radiologically normal brains without history of neuropsychological disorder. Among these, 6 subjects (3 females) had participated in a prior study in which we localized thin- and thick-type columns in areas V2/V3 (Nasr et al., 2016; Nasr and Tootell, 2016). However, data reported here are based on independent scan sessions, using an independent set of stimuli (see below). All experimental procedures conformed to NIH guidelines and were approved by Massachusetts General Hospital protocols. Written informed consent was obtained from all subjects prior to the experiments.

2.2. General procedures

Each subject was scanned in a high field scanner (Siemens 7T whole-body system, Siemens Healthcare, Erlangen, Germany) to localize their thin-type (color-selective) and thick-type (stereo-selective) columns, in 2 sessions each, on different days. Hue-specific responses were measured in two additional sessions. All 7 subjects were also scanned in a 3T scanner (Tim Trio, Siemens Healthcare) in two additional sessions, for structural and retinotopic mapping, and to localize occipital temporal color-selective area(s). Thus for each subject, data was based on at least eight scan sessions.

2.3. Visual stimuli and procedure

Experimental stimuli included four hue-varying gratings: two end-spectral (blue-gray and green-gray) gratings, and two mid-spectral (i.e. yellow-gray, and red-gray) gratings, plus achromatic (gray level) luminance-varying sinusoidal gratings, each presented in independent blocks. All gratings were matched in mean luminance via flicker photometry (see below) for each subject; thus the hue-varying gratings were 'isoluminant'. The dominant wavelengths of the blue, green, yellow and red hues were near 463, 547, 572 and 612 nm, respectively. All stimuli subtended $20^\circ \times 20^\circ$ of visual angle. Each hue-varying grating was presented in independent blocks. The spatial frequency of all

gratings was low (0.3 cycle/°), to tap the relatively higher sensitivity to color (relative to luminance) sensitivity at low spatial frequencies (van der Horst and Bouman, 1969; Granger and Heurtley, 1973), and to minimize linear chromatic aberration (i.e. luminance artifacts) at color borders. Stimulus examples are shown in Fig. 1.

In each subject, the mean luminance level was equated for each hue-varying grating. Specifically, mean luminance values for red, yellow, green, and achromatic gray were defined based on the method of flicker photometry (Ives, 1907; Bone and Landrum, 2004; Nasr et al., 2016). The luminance for all hues was set to the limiting (maximum) luminance for blue (i.e. 4.8 Ft.-L.) (see below). The isoluminance adjustment was conducted independently in each session inside the scanner, prior to each functional scan session.

Isoluminant values are known to vary with stimulus eccentricity (Mullen, 1985; Livingstone and Hubel, 1987; Bilodeau and Faubert, 1997; Nasr et al., 2016). Accordingly, flicker photometry measurements were conducted independently across three different eccentricities (foveal (0°–2°), parafoveal (2°–5°), and peripheral (5°–10°)) relative to the maximum blue luminance at each eccentricity. Table 1, Tables S1 and S2 show the resultant values across the three eccentricities, averaged over the seven subjects in CIE-Lab, LMS and DKL color-coordinate systems. Resulting values were extrapolated between these three sampled eccentricities by fitting a logarithmic function.

During the scans, stimuli were presented via a projector (Sharp XG-P25X, 1024 × 768 pixel resolution, 60 Hz refresh rate) onto a rear-projection screen, viewed through a mirror mounted on the receive coil array. MATLAB 2017a (MathWorks, Natick, MA, USA) (RRID: SCR_001622) and the Psychophysics Toolbox (Brainard, 1997; Pelli, 1997) were used to control stimulus presentation. In different blocks, grating stimuli were presented at horizontal and vertical orientations, drifting in orthogonal directions (reversed every 6 s) at 4°/s. Each run included 10 stimulus presentation blocks (24 s per block), beginning and ending with an additional block (18 s) of uniform gray. Each subject participated in 12 runs per session, during which 1104 functional volumes were collected (see Imaging section below). During the scans, subjects conducted a 'dummy' attention task which required subjects to maintain fixation on a very small central target, and report small changes in the target color.

Table 1
Isoluminance hues (mean ± s.d.) across the three eccentricities, in CIE-Lab color space, estimated based on the method of flicker photometry.

		Foveal	Parafoveal	Peripheral
Red	L	31.22 ± 1.82	36.92 ± 3.21	43.37 ± 3.37
	a	54.65 ± 2.10	61.24 ± 3.71	68.70 ± 3.91
	b	45.03 ± 2.12	51.20 ± 3.45	57.62 ± 3.32
Green	L	32.15 ± 7.41	35.94 ± 7.48	42.49 ± 9.74
	a	−40.00 ± 6.16	−43.15 ± 6.21	−48.59 ± 8.09
	b	38.25 ± 6.58	41.52 ± 6.21	46.84 ± 7.91
Yellow	L	34.62 ± 7.57	38.46 ± 7.36	42.53 ± 7.62
	a	−9.64 ± 1.44	−10.37 ± 1.40	−11.15 ± 1.45
	b	41.98 ± 6.80	45.38 ± 6.31	48.85 ± 6.43
Gray	L	20.85 ± 6.75	30.17 ± 7.07	37.62 ± 6.80
	a	0 ± 0.0010	0 ± 0.0011	0 ± 0.0010
	b	0 ± 0.0004	0 ± 0.0004	0 ± 0.0004

2.4. Localization of regions of interest

Main regions of interest (ROIs) included the peripheral representation (3–10°) of the V1, V2 and V3 (measured across the retinotopically-activated portion of each area (see below)), plus thin-type and thick-type columns within each of V2 and V3 (see below). In addition, a ROI was defined for area V3A as a control (non-color-selective) region (Mullen et al., 2007; Brouwer and Heeger, 2009; Tootell and Nasr, 2017). In four subjects, our field of view (FOV) also included the occipital temporal color-selective area, as described earlier at lower spatial resolution (Hadjikhani et al., 1998; Bartels and Zeki, 2000; Wade et al., 2002; Lafer-Sousa et al., 2016).

Borders of areas V1, V2, V3 and V3A were defined retinotopically in each individual subject. Stimuli used for retinotopic mapping were color images of scenes and face mosaics, presented within retinotopically limited apertures, against a gray background. These retinotopic apertures included horizontal and vertical meridian wedges (radius = 10°, polar angle = 30°), a foveal disk (radius = 0–1.5°) and a peripheral ring (radius = 4.5–10°). Further details are reported elsewhere (Sereno et al.,

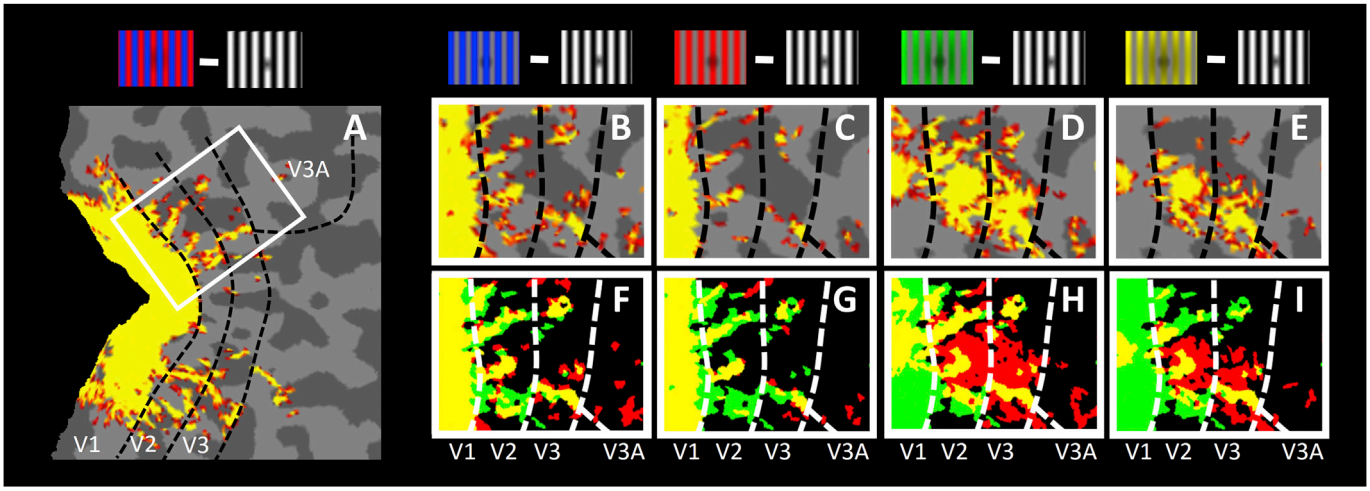

Fig. 1. Activity maps evoked by hue-varying (relative to luminance-varying) gratings in striate and extrastriate cortex, in one hemisphere. **A)** Localization of thin-type (color-selective) columns within extrastriate visual areas V2 and V3, produced by contrasting the activity evoked by color-varying vs. luminance-varying stimuli (red-to-yellow: $p < 10^{-3}$ to $p < 10^{-6}$), as defined previously (Nasr et al., 2016). This stimulus contrast evoked a relatively uniform activity pattern within V1 (at this spatial resolution), and also activated thin-type columns within V2 and V3. Stimulus examples are shown above the panels. The area defined by the white outline in panel A is enlarged and used in the remaining panels. **B-E)** Selective activity evoked by blue-gray, red-gray, green-gray and yellow-gray gratings relative to luminance-varying stimuli (red-to-yellow: $p < 0.05$ to $p < 10^{-3}$), respectively. **F-I)** Non/overlap of activity in thin-type columns relative to activity evoked selectively by each different hues (green: supra-threshold activity produced by the color-selective localizers (as in panel **A**); red: supra-threshold selective activity produced by each different hues; yellow: overlap between color-selective and hue-related response; black: no activity). Thresholds are defined as in panels **A-E**. Overall, the activity driven by spectrally extreme hues (i.e. red and blue) was largely confined to thin-type columns. In contrast, activity evoked by mid-spectral hues (i.e. green and yellow) extended well beyond thin-type columns. In all maps, borders of visual areas were defined retinotopically in an independent scan session (see Methods).

1995; Tootell et al., 1997; Nasr et al., 2011).

Additional scan sessions (with a >7 day gap with the main tests) localized thick-type and thin-type columns within V2 and V3, as described previously (Nasr et al., 2016; Nasr and Tootell, 2016; Tootell and Nasr, 2017). Briefly, thin-type columns were localized by contrasting the activity evoked by isoluminant red-blue relative to luminance-varying gratings (Fig. 1). Thick-type columns were localized by contrasting the activity evoked by depth-varying (−0.2° to 0.2°) random dot stereograms (RDS (Julesz, 1971)) relative to the same dot array moving within the fronto-parallel plane. The occipital temporal color-selective site was localized based on a conventional (color-varying vs. luminance-varying) stimulus contrast (Hadjikhani et al., 1998).

2.5. Imaging

Main experiments were conducted in a 7T Siemens whole-body scanner equipped with SC72 body gradients (70 mT/m maximum gradient strength and 200 T/m/s maximum slew rate), using a custom-built 32-channel helmet receive coil array and a birdcage volume transmit coil (Keil et al., 2010). Voxel dimensions were prescribed at 1.0 mm, isotropic. Single-shot gradient-echo EPI was used to acquire functional images with the following protocol parameter values: TR = 3000 ms, TE = 28 ms, flip angle = 78°, matrix = 192 × 192, BW = 1184 Hz/pix, echo-spacing = 1 ms, 7/8 phase partial Fourier, FOV = 192 × 192 mm, 44 oblique-coronal slices, acceleration factor $R = 4$ with GRAPPA reconstruction and FLEET-ACS data (Polimeni et al., 2015) with 10° flip angle.

Voxel size estimation might be affected by 1) pulsatility artifacts, plus 2) the draining vein effect of the underlying vasculature. To minimize the impact of draining veins, we used a differential stimulation paradigm (Yacoub et al., 2008) and also by sampling far from the pial surface (Polimeni et al., 2010; Nasr et al., 2016). The impact of pulsatility artifacts in human occipital lobe is expected to be approximately 90 microns (Enzmann and Pelc, 1992; Poncelet et al., 1992). With regard to ~7 mm distance (center-to-center) between human thin-type stripes (Nasr et al., 2016), these artifacts should not have a major impact on our measurements.

For optimal comparison to prior data, the retinotopic mapping, and the localization of the occipital temporal color area, were conducted using a 3T Siemens scanner (Tim Trio) and a Siemens 32-channel receive coil array. This functional data was acquired using single-shot gradient-echo EPI. Voxels were prescribed at 3.0 mm (isotropic) using the following protocol parameters: TR = 2000 ms, TE = 30 ms, flip angle = 90°, matrix = 64 × 64, BW = 2298 Hz/pix, echo-spacing = 0.5 ms, no partial Fourier, FOV = 192 × 192 mm, 33 axial slices covering the entire brain, and no acceleration. As reported previously (Nasr and Tootell, 2016), for one subject, these retinotopic maps (at 3T) were compared to the maps collected in a 7T scanner, showing essentially identical borders at both field strengths, as expected (Olman et al., 2010).

Structural (anatomical) data were acquired using a 3D T1-weighted MPRAGE sequence with protocol parameter values: TR = 2530 ms, TE = 3.39 ms, TI = 1100 ms, flip angle = 7°, BW = 200 Hz/pix, echo spacing = 8.2 ms, voxel size = 1.0 × 1.0 × 1.33 mm^3, FOV = 256 × 256 × 170 mm^3.

2.6. Data analysis

Functional and anatomical MRI data were pre-processed and analyzed using FreeSurfer and FS-FAST (version 5.3; http://surfer.nmr.mgh.harvard.edu/) (RRID:SCR_001847) (Fischl, 2012). For each subject, inflated and flattened cortical surfaces were reconstructed based on the high-resolution anatomical data (Dale et al., 1999; Fischl et al., 1999, 2002). All functional images were corrected for motion artifacts. 3T functional data were spatially smoothed (Gaussian filtered with a 5 mm FWHM), but no spatial smoothing was applied to the main imaging data acquired at 7T (i.e. 0 mm FWHM). For each subject, functional data from each run were rigidly aligned (6 DOF) relative to his/her own structural scan, using rigid Boundary-Based Registration (Greve and Fischl, 2009). This procedure made it possible to combine (average) data acquired across multiple scan sessions, for each subject.

A standard hemodynamic model based on a gamma function was fit to the fMRI signal to estimate the amplitude of the BOLD response. For each individual subject, the average BOLD response maps were calculated for each condition (Friston et al., 1999). Then, voxel-wise statistical tests were conducted by computing contrasts based on a univariate general linear model. The resultant significance maps were projected onto the subject's anatomical volumes and reconstructed cortical surfaces.

To reduce the impact of pial veins on evoked activity maps (Yacoub et al., 2008; Polimeni et al., 2010; Nasr et al., 2016), brain activity was sampled from the deepest cortical layer. Specifically, for each subject, the gray-white matter (deep) interfaces were defined based on each subjects' own high-resolution structural scans using FreeSurfer (Dale et al., 1999; Fischl et al., 1999, 2002). To measure the fMRI activity, the percent fMRI signal change was calculated for those functional voxels that intersected this gray-white matter interface, and the resultant values were projected onto the corresponding vertices of the surface mesh.

2.7. Statistical analysis

Statistical tests were based on repeated measures ANOVA. When necessary (based on Mauchly test), results were corrected for violation of the sphericity assumption using the Greenhouse-Geisser method. To test the reliability of the potential effects, a group factor (first vs. second scan) was also considered in all ANOVA tests. We did not observe any between-hemisphere difference (i.e. laterality). Accordingly, in all ROI analyses, data from the opposite hemispheres were averaged together to increase the signal to noise ratio. In all cases, data were tested for normality before choosing the statistical test: $p < 0.05$ was considered significant. All statistical analyses were conducted using the MATLAB (2017a) statistics and machine learning toolbox (MathWorks, Natick, MA, USA).

3. Results

In previous studies (Nasr et al., 2016; Tootell and Nasr, 2017), we used two-hue sinusoidal gratings (i.e. alternating red and blue stimulus ‘stripes’) to localize ‘thin-type’ (color-selective) columns within human V2 and V3 (see Methods). Here, our goal was to test the independent responses evoked by end-spectral (red and blue) and mid-spectral (green and yellow) hues and achromatic luminance-varying gratings (Fig. 1) in areas V1, V2 and V3, plus the more occipital temoral color-selective sites described previously (Hadjikhani et al., 1998; Bartels and Zeki, 2000; Wade et al., 2002; Brewer et al., 2005; Brouwer and Heeger, 2009; Lafer-Sousa et al., 2016). While subjects continuously viewed these stimuli, high-resolution fMRI data was collected using a 7T scanner, in 7 human subjects. To test the reliability of our findings, and to improve the signal quality in each individual subject, all subjects were scanned in two scan sessions, on different days (see Methods).

3.1. Activity produced by end-spectral hues

Partly as a comparison to the red-blue gratings used as localization stimuli (Nasr et al., 2016), we first analyzed the selectivity maps evoked by each end-spectral hue (i.e. red-gray and blue-gray) and compared the resultant maps relative to each other, and relative to the selectivity maps evoked by the dual-hue localization grating (Nasr et al., 2016).

Fig. 1 shows the response to red-blue (Fig. 1A), blue-gray (Fig. 1B) and red-gray (Fig. 1C) stimuli in one hemisphere. All these maps showed strong activity within striate cortex (V1), which was topographically unclustered at this spatial resolution and threshold. As expected from previous studies in both humans (Nasr et al., 2016) and monkeys (Tootell et al., 2004), the blue-gray and red-gray gratings (vs. the achromatic luminance-varying grating) produced stripe-shaped activity which

radiated perpendicularly to the V1-V2 border, extending across the stimulated extent of area V2 and V3. These activity maps evoked by the single-hue (red-gray and blue-gray) gratings showed considerable overlap with the thin-type columns, as activated by dual-hue (i.e. red-blue) localizing gratings (Fig. 1F and G) and at these thresholds, it did not extend into thick-type columns (Fig. 2A–B), localized based on their disparity-selective response (see Methods). This data is broadly consistent with many prior studies in NHPs that have reported V2 thin-type (but not thick-type) stripes to be 'color-selective' (Livingstone and Hubel, 1984; Xiao et al., 2003; Tootell et al., 2004; Lu and Roe, 2008). Contrasting the response evoked by red-gray vs. blue-gray did not evoke any significant difference at this threshold ($p < 0.05$). Fig. S1A shows additional examples of activity maps evoked by end-spectral hues.

3.2. Activity produced by mid-spectral hues

Consistent with previous reports in non-human primates (Vautin and Dow, 1985; Creutzfeldt et al., 1987; Tootell et al., 1988; Salzmann et al., 2012), we found that the mid-spectral (i.e. green and yellow) single-hue gratings produced activity maps that differed strikingly from the pattern of activity produced by end-spectral (red and blue) hues (Fig. 1D and E) as described above. First, in area V1, the isoluminant mid-spectral hues produced much weaker activity, compared to that produced by the end-spectral hues. However, in extrastriate areas V2 and V3, the two mid-spectral hues produced strong activity maps. Secondly, in contrast to the stripe-shaped activity maps evoked by end-spectral hues, activity evoked by mid-spectral hues was distributed relatively uniformly across V2 and V3. In other words, the activity produced by mid-spectral hues extended well beyond the thin-type columns, into the thick-type columns (see Methods and Fig. 2C), consistent with prior single unit data in monkeys (Yoshioka and Dow, 1996; Yoshioka et al., 1996). Contrasting the response evoked by green-gray vs. yellow-gray did not evoke any significant difference at this threshold ($p < 0.05$). Fig. S1B shows further examples of activity maps evoked by mid-spectral hues. Importantly, since all the single-hue maps were collected in random order within each scan session, this result cannot be attributed to uncontrolled differences across scan sessions, and/or a difference in signal to noise ratio.

3.3. Direct comparison of activity maps evoked by end-vs. Mid-spectral hues

The above single-hue activity maps suggested significant differences between hue preferences in striate vs. early extrastriate cortex. To test this more directly, we compared the activity maps evoked by the contrast between end-vs. mid-spectral hues. As demonstrated in Fig. 2, these activity maps confirmed the observations based on the single-hue maps described above (Fig. 1). Specifically, V1 showed a relatively stronger preference for end-spectral hues, whereas activity in V2 and V3 was more strongly driven by mid-spectral (rather than end-spectral) hues, driven mainly by a significant response to mid-spectral (rather than end-spectral) hues outside thin-type columns (Fig. 2D). This effect was observed in both dorsal and ventral portion of areas V2 and V3 (Fig. S2).

Thus, in both the single-hue and combined-hue analyses, the preference for mid-spectral hues was not limited to the thin-type columns (as defined previously in response to red-blue, blue-gray or red-gray gratings); instead this bias for mid-spectral hues was also evident beyond thin-type columns, including thick-type columns (Fig. 2D). Here again, this effect was confirmed in all individuals at the level of activity maps (Fig. 3 and Fig. S3). Further quantitative analysis of this bias is included in section 3.5.

3.4. Quantitative analysis of overlap

It could be argued that our choice of threshold level influenced the amount of overlap between the single-hue activity maps and thin-type columns (Fig. 1 and Fig. S1). To address this possibility, we measured the percentage overlap between these maps and thin-type columns (see Methods (section 2.4)), across a wide range of threshold levels (i.e. $p = 0.05$ to 10^{-7}). As a control condition, we also measured the level of topographical overlap between these hue maps and thick-type (see Methods (section 2.4)) columns, across the same range of thresholds.

Fig. 4 shows the results. We applied four independent two-way repeated measures ANOVA ('threshold' and 'column-type' (thin-type vs. thick-type)) to the measured levels of overlap between activity maps evoked by 'blue-gray' and 'red-gray' stimuli and thin/thick columns located within V2 and V3. In both V2 and V3, the activity maps evoked by end-spectral hues showed significantly more overlap with thin-type rather than thick-type columns ($F(1, 6) > 18.50$, $p < 0.01$), across all tested thresholds. We also found a significant interaction between 'column-type × threshold' ($F(11, 66) > 18.25$, $p < 0.01$), consistent with a more selective overlap between these maps and thin-type columns at higher threshold levels. All tests of repeated measures ANOVA were corrected for violation of the sphericity assumption (see Methods).

In contrast, maps evoked by mid-spectral hues showed considerable overlap with both thin-type and thick-type columns (Fig. 5). Application of the tests described above showed only a significant effect of 'column-type × threshold' interaction, in response to single-hue green-gray stimuli ($F(11, 66) = 7.93$, $p = 0.02$), in V3. The effects of 'column-type'

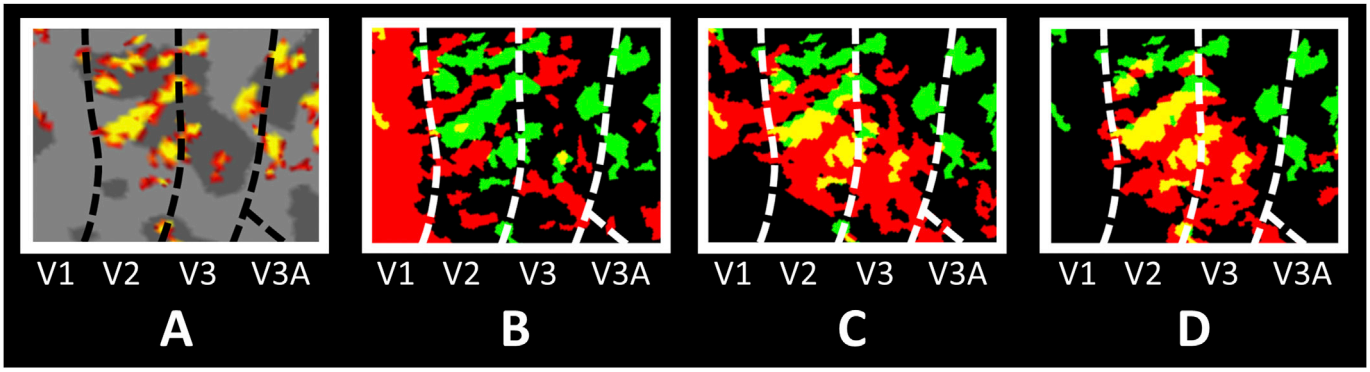

Fig. 2. Co-localization of activity maps evoked by mid- and end-spectral hues relative to thick-type stripes/columns within V2 and V3. **A)** Localization of thick-type columns based on their disparity-selective response (Nasr et al., 2016). **B)** Co-localization of thick-type columns relative to the activity map evoked selectively by end-spectral (averaged over red-gray and blue-gray) relative to luminance-varying stimuli. This map did not show any apparent overlap with thick-type columns. **C)** Co-localization of thick-type columns relative to the activity map evoked selectively by mid-spectral (averaged over green-gray and yellow-gray) relative to luminance-varying stimuli. In contrast to end-spectral stimuli, activity evoked selectively by mid-spectral stimuli showed a considerable overlap with thick-type columns in V2 and V3. **D)** Co-localization of thick-type columns relative to the activity map evoked by 'mid- > end-spectral' contrast. All other details are similar to Fig. 1.

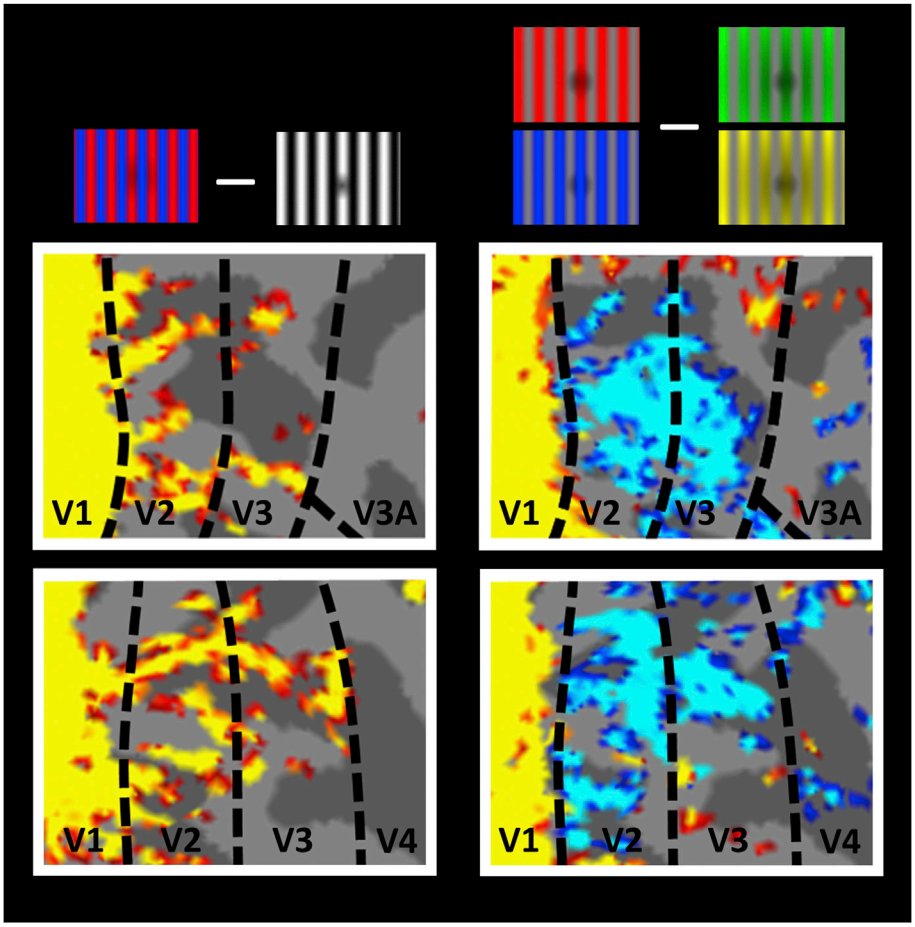

Fig. 3. Activity map in response to spectrally extreme vs. mid-spectral hues, relative to the localization map of thin-type columns in one hemisphere. Top and bottom rows demonstrate the activity maps from dorsal and ventral portion of the same hemisphere. In striate cortex (V1), spectrally extreme hues evoked a stronger response, relative to mid-spectral hues. This bias was reversed in extrastriate areas V2 and V3, in which mid-spectral hues evoked a stronger response compared to spectrally extreme hues. This V2/V3bias extended beyond the thin-type columns without any apparent difference between dorsal vs. ventral regions. Other details are as in Fig. 1.

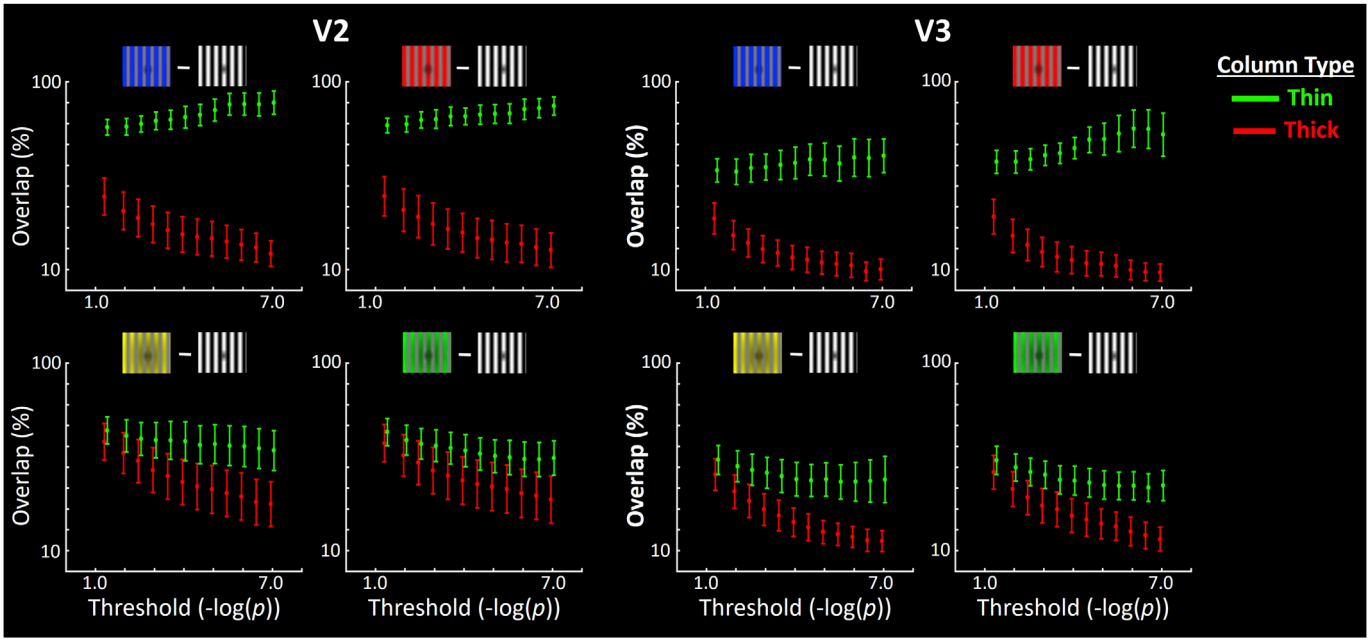

Fig. 4. Extent of overlap between the activity evoked by each hue, relative to thin-type vs. thick-type columns within V2 and V3, across a range of thresholds. Data is combined from (averaged across) all subjects. In both V2 and V3, activity evoked by spectrally extreme hues (top row) showed more overlap with thin-type (green) rather than thick-type (red) columns. In contrast, activity evoked by mid-spectral hues (bottom row) included considerable overlap with thick-type columns. All activity was measured relative to the activity evoked by luminance-varying stimuli. Error bars represent 1 standard error.

F(1, 6)<5.94, $p>0.05$ and 'column-type × threshold' (F(11, 66)<3.56, $p>0.09$) in all other tests remained marginally insignificant. This data confirmed that activity maps evoked by mid-spectral hues extended well beyond thin-type columns into thick-type columns, across a wide range of thresholds.

To directly test the interaction between 'hue' (red vs. yellow vs. green vs. blue) and column-type (thin-type vs. thick-type), we applied a three-way repeated measures ANOVA ('hue', 'column-type' and 'threshold') to activity maps within V2 and V3. As expected from the individual tests described above, in V2 and V3 we found a significant interaction between the effects of 'column-type × hue' (F(3, 18)>12.89, $p < 10^{-4}$) and 'column-type × hue × threshold' (F(33, 198)>3.49, $p < 0.04$). This result further confirms that the level of activity extension may vary depending on the stimulus hue (dominant wavelength) of stimulus hues.

3.5. Analysis of hue preference within regions of interest

To further test for biases in hue preference, we compared the level of color-selective BOLD signal evoked by each of these four stimuli, relative to the activity evoked by luminance-varying stimuli (Fig. S4) within different regions of interest (ROIs), including V1 and thin- and thick-type columns in V2 and V3 (see Methods (section 2.4)). As expected from the above results, in V1, end-spectral (blue and red) hues evoked higher responses compared to mid-spectral (green and yellow) hues (Fig. 5A). Specifically, application of one-way repeated measures ANOVA (hue (red vs. blue vs. green vs. yellow)) with a group factor (session 1 vs. 2) showed a significant effect of 'hue' (F(3, 36) = 45.69, $p < 10^{-6}$), without any significant 'hue × session' interaction (F (3, 36) = 0.64, $p = 0.51$). These results confirmed a reliable preference for the end-spectral hues in V1, compared to the mid-spectral hues.

At the spatial scale of areas, V2 and V3 showed an opposite bias for mid-spectral hues (Fig. 5B). At a finer spatial scale, V2/V3 thin-type columns showed a strong response to all tested hues, including a significantly higher response to mid-spectral hues compared to luminance-varying stimuli (Fig. 5C–D). Although thick-type columns also showed a selectively higher response to the mid-spectral hues (compared to luminance-varying stimuli), response of thick-type columns to end-spectral hues was essentially equivalent to their response to achromatic luminance-varying gratings. Two independent applications of two-way repeated measures ANOVA (hue (red vs. blue vs. green vs. yellow) and column-type (thin-vs. thick-type)) with a group factor (session 1 vs. 2) to the measured color-selective responses in V2 and V3 showed a significant effect of 'hue' (F(3, 36)>12.93, $p < 10^{-3}$) and 'column-type' (F(1, 12)> 100.56, $p < 10^{-6}$) in both areas. Here again, we found no interaction between the effects of scan session and the other two independent factors (F<1.35, $p>0.26$), consistent with high reliability in the results across scan sessions. Thus, relative to the luminance-varying grating baseline, the mid-spectral hues evoked strong activity in both thin- and thick-type columns, while end-spectral hues evoked strong activity only within thin-type columns.

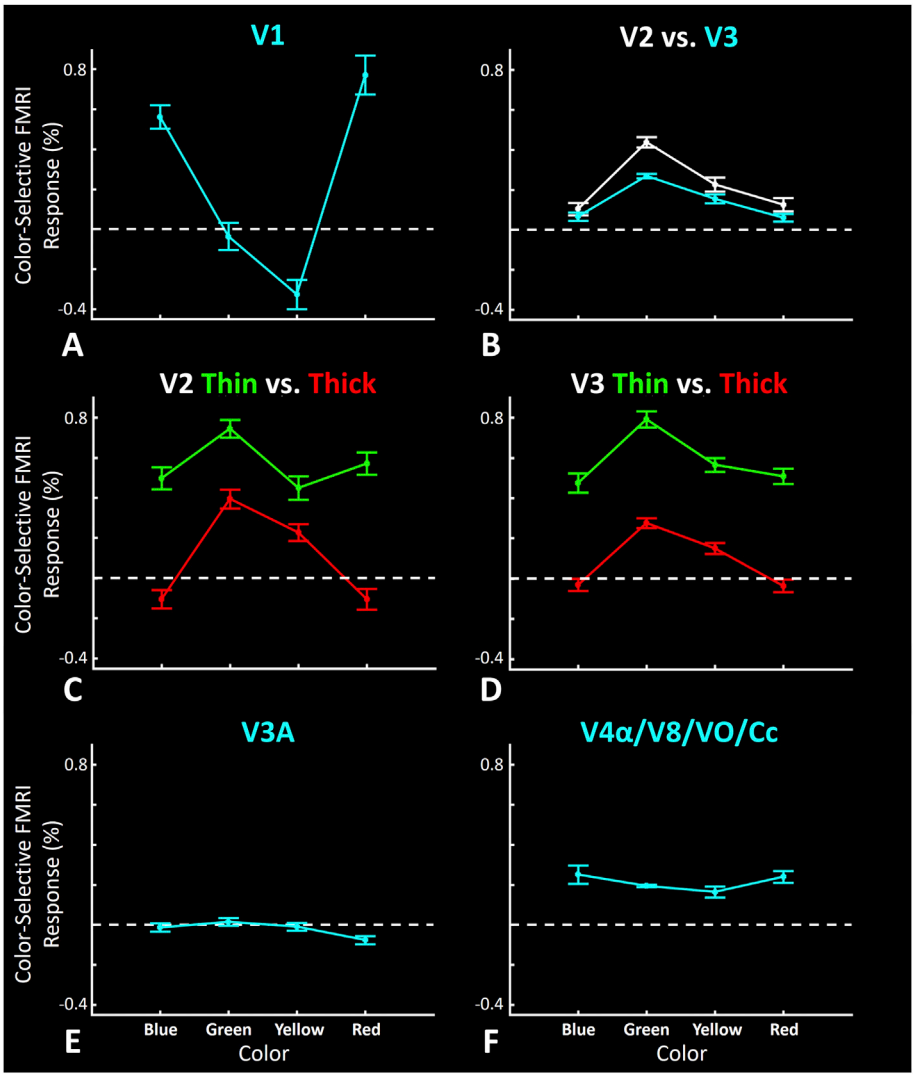

Fig. 5. FMRI activity evoked in different regions of interest (ROIs) by blue-gray, green-gray, yellow-gray and red-gray gratings, measured relative to the activity evoked by luminance-varying gratings. **A)** V1 showed a strong activity bias for spectrally extreme hues. In fact, activity produced by mid-spectral hues was not 'color-selective', relative to the activity produced by luminance-varying gratings. **B)** In contrast, whole-area measurements of V2 and V3 (lower left panel) showed an opposite bias, favoring mid-spectral hues. **C-D)** At a finer (i.e. columnar) spatial scale, V2/V3 thin-type columns (middle panels) responded to all hues, while thick-type columns responded only to mid-spectral hues. Thus, the mid-spectral hue preference in the V2/V3 response was reflected in the activity within thick-rather than thin-type columns. **E)** Area V3A (top right) did not show any color-selective response. **F)** The occipitotemporal 'color-selective' site (V4α/V8/VO/Cc) responded equivalently to all hues. Error bars represent 1 standard error.

As evident in the activity maps (e.g. Fig. 1), our ROI analysis did not reveal any color-selective activity in area V3A. In V3A, application of one-way repeated measures ANOVA (as applied to V1) did not show any significant effect of 'hue' ($F(3, 18) = 1.79$, $p = 0.20$) and/or 'hue × session' ($F(3, 36) = 0.36$, $p = 0.78$). Thus, consistent with previous reports (Mullen et al., 2007; Brouwer and Heeger, 2009; Tootell and Nasr, 2017), activity in V3A was apparently insensitive to variations in stimulus hue, as well as to color *per se* (i.e., relative to luminance).

3.6. Activity within occipital temporal color-selective area

In 4 subjects, our slice prescription included the color-selective site located in the occipital temporal cortex (see Methods (section 2.4)), specifically in the fusiform gyrus, posterior to the medial fusiform sulcus (Fig. 6). Previously this site has been described as 'color-selective' based on conventional fMRI, termed either 'V4α' (Bartels and Zeki, 2000) or 'V8' (Hadjikhani et al., 1998), or 'VO' (Wade et al., 2002; Brewer et al., 2005) or 'Cc' (Lafer-Sousa et al., 2016). Consistent with that earlier data, we found color-selective activity within this site (Fig. 6). Despite some inter-subject variability in the anatomical location of this site, this color-selective activity also remained significant in the group-average activity maps (Fig. S5) as suggested previously by other studies in a larger pool of subjects (see above). Thus, at least part of the variability between subjects arose from anatomical factors, rather than functional factors.

However, in contrast to the activity in the more posterior (presumably lower-stage) visual areas (V1, V2, V3, and V3A), this occipital temporal color-selective site showed no strong hue bias; instead we found a statistically equivalent response to all four hues (Fig. 5F) and application of the analysis described above did not show any significant effect of 'hue' ($F(3, 18) = 1.01$, $p = 0.37$) and/or 'hue × session' interaction ($F(3, 18) = 0.28$, $p = 0.70$).

To further test whether this change in hue preference (from biased to unbiased, relative to the perception) was statistically significant, we applied a two-factor repeated measures ANOVA (hue (red vs. yellow vs. green vs. red) and area (V2 thin-type vs. V3 thin-type vs. anterior site) with a group factor (session 1 vs. 2) to activity measured for the 4 subjects in which our FOV also included the anterior color-selective site. Despite the limited number of subjects ($n = 4$) in this test, we found a significant effect of 'area' ($F(2, 12) = 15.30$, $p < 10^{-3}$) and more importantly a significant 'area × hue' interaction ($F(6, 36) = 5.18$, $p = 0.02$), without any significant effect of group and/or interaction between this factor and other independent factors ($p > 0.16$). Consistent with a previous report (Brouwer and Heeger, 2009), this data suggests that hue preference is essentially equivalent across different hues in this higher level site.

Interestingly, in one of these four subjects, we also found preliminary evidence of segregated clusters within this occipital temporal area that were selectively activated by mid-vs. end-spectral hues (Fig. S6). This supports the general finding of a segregation of color hues along the mid-vs. end-spectral categories, as described above in V2 and V3 (Figs. 1 and 3). However, because of sampling limitations, more such data is required before more solid conclusions can be reached.

3.7. Response to second-, third- and fourth-preferred hues

The above activity maps highlight the preferred hue in each vertex. Here we further tested whether the second-, third- and fourth-preferred hues could also evoke a significant color-selective response (i.e. stronger than the response evoked by luminance-varying stimuli), in each vertex.

As demonstrated in Fig. 7, the first- ($t(6) = 6.13$, $p < 10^{-3}$) and the second-preferred hues ($t(6) = 3.79$, $p < 0.01$), but not the third- ($t(6) = 0.05$, $p = 0.95$) and fourth- ($t(6) = 2.16$, $p = 0.07$) preferred ones, evoked a significant response within V1. In contrast to V1, thin-type vertices within V2 and V3 showed a significant response even to their third- and fourth-preferred hues ($t(6) > 2.65$, $p < 0.03$), suggesting that they have a broader preference (i.e. less/weaker hue-selectivity) compared to V1. To test this difference between V1 vs. V2/V3 thin-stripes more directly, we applied a two-way repeated measures ANOVA (order (first vs. second vs. third vs. fourth) and area (V1 vs. V2 thin-type columns vs. V3 thin-type columns)) to the measured activity within these regions. The results yielded significant effects of 'order' ($F(3, 18) = 188.53$, $p < 10^{-5}$), 'area' ($F(2, 12) = 7.43$, $p = 0.02$) and 'order × area' ($F(6, 36) = 8.69$, $p = 0.02$). Since the amplitude of the color-selective responses evoked by the first preferred hue was comparable between V1, V2 and V3, this difference in response profile could not be linked to the stronger color-selectivity of extrastriate cortex, compared to striate cortex.

In thick-type vertices, we found a significant response to only the first and the second preferred hues ($t(6) > 3.49$, $p < 0.01$) (Fig. 7). Thus, compared to thin-type columns, thick-type columns within V2 and V3

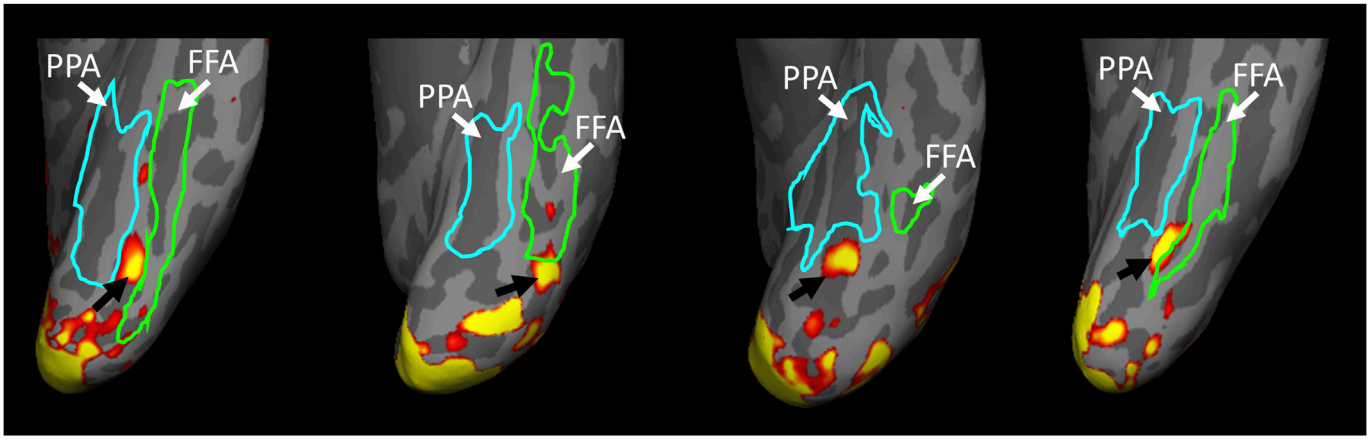

Fig. 6. Localization of the anterior occipito-temporal color-selective site (V4α/V8/VO/Cc), based on contrasting activity evoked by color-vs. luminance-varying gratings (Hadjikhani et al., 1998; Wade et al., 2002) in 4 different hemispheres (red to yellow: $p < 10^{-3}$ to $p < 10^{-6}$). For comparison, the nearby Fusiform Face Area (FFA; green outline) (Kanwisher et al., 1997) and the Parahippocampal Place Area (PPA, cyan outline) (Epstein and Kanwisher, 1998) were also localized in each subject by contrasting activity evoked by presenting faces and scenes ($p < 10^{-3}$) in a separate scan session. Details of these scans have been reported previously elsewhere (Nasr et al., 2011). Thresholds for both areas were $p < 10^{-3}$. Details of the FFA and PPA localization are reported elsewhere (Nasr et al., 2011). Consistent with a recent report (Lafer-Sousa et al., 2016), the color-selective site (black arrow) was located immediately posterior to the mid-fusiform sulcus, and posterior to FFA and PPA, in all subjects/hemispheres. All panels show a ventral view of the cortical surface. Posterior in the brain is lower in the figure, and medial is to the left.

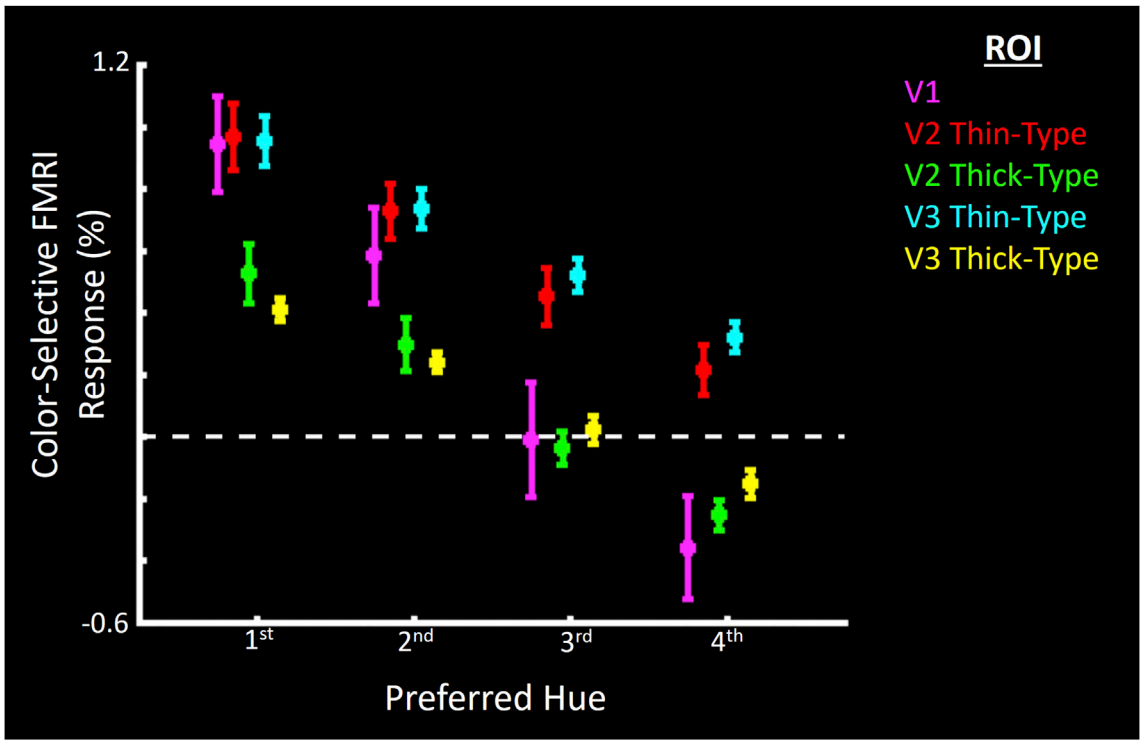

Fig. 7. Activity evoked by the first-, second-, third- and forth-preferred hues, averaged over vertices within different ROIs. All activity was measured relative to the luminance-varying stimuli. In the thin-type columns, first-through fourth-preferred hues evoked a stronger response relative to the luminance-varying stimuli ($p < 0.03$). In contrast, in V1 and thick-type columns, only the first two preferred hues evoked a significantly selective response ($p < 0.01$). Error bars represent 1 standard error.

showed more restricted hue selectivity. However, this effect could reflect (at least partly) the weaker overall color-selectivity in these ROIs compared to thin-type columns.

4. Discussion

Based on the three axes on which light can vary (hue, saturation and luminance), a common approach in studying the neural response to different hues has been to reduce the contribution of luminance by using isoluminant stimuli generated based on the method of flicker photometry (see Methods). Based on a similar approach, we found that color-selective sites in thin-type columns in V2, V3, and occipital-temporal cortex all responded essentially equally to all four isoluminant hues.

However, elsewhere in early visual cortex (thick-type columns in V2/V3, and in V1), our results revealed strikingly different fMRI response amplitudes to the four hues tested. Some of these hue response differences were consistent with an intriguing (albeit largely ignored) model in the literature, designed in part to explain how the visual system can maximize spatial resolution by minimizing chromatic aberration (Dow, 2002). Another response bias that we found (in V1) was more empirical in nature: although this bias has been reported in multiple studies (Tootell et al., 1988; Yoshioka and Dow, 1996; Salzmann et al., 2012), it has not yet been linked to a specific model of color processing. In any event, both of these hue biases indicated differences in cortical processing along the dimension of end-vs. mid-spectral processing, across both the area and columnar spatial scales.

4.1. Area-scale findings

At the spatial scale of cortical areas, a striking difference in hue preference was found in V1, compared to that in cortical areas V2 and V3. Specifically, V1 showed a preference for end-spectral (red and blue) hues, whereas V2 and V3 responded preferentially to mid-spectral hues (green, and often yellow). Thus for one thing, the spectral bias in extrastriate cortex was not a passive, downstream version of the bias in striate cortex.

Consistent with these findings in humans, previous studies of V1 in non-human primates also described a strong bias for red and blue hues, based on electrophysiology (Creutzfeldt et al., 1987; Yoshioka and Dow, 1996), optical recording (Salzmann et al., 2012), and deoxyglucose mapping (Tootell et al., 1988). It was speculated that this V1 bias is related to perceptual measurements of color saturation, in which sensitivity also varies fundamentally between mid- vs. end-spectral hues (Tootell et al., 1988). However, a preliminary experiment produced only partial support that idea (Tootell et al., 1988).

Unexpectedly, we also found a weaker but reversed hue bias for mid-spectral (relative to end-spectral) hues in V2 and V3, at the area level. At least part of this difference could be due to the steeper contrast response function of V2/V3 compared to V1 (Hall et al., 2005; Breitmeyer et al., 2018). Specifically, as indicated in Table S2, our end-spectral hues contained a higher 'total color contrast' compared to mid-spectral hues. For that reason, it could be argued that this difference leads to a higher color-selective response by end-compared to mid-spectral hues in V1. However, the relatively sharp change in color-contrast response, and especially the reversal of the response function (Fig. 5A–B) between V1 and V2/V3, are inconsistent with this interpretation (see below).

Much prior evidence suggests that dorsal stream areas (e.g. V3A, MT) dominated by magnocellular pathways are comparatively insensitive to color variations (Hadjikhani et al., 1998; Mullen et al., 2007; Brouwer and Heeger, 2009; Tootell and Nasr, 2017). Our current data support that conclusion, at least in V3A which was included in our scanning prescription (Fig. 5).

4.2. Hue preference in thin- and thick-type columns

At the smaller spatial scale of columns, we found significant differences in the hue preference within V2 and V3. For instance, V2-V3 biases

for mid-spectral hues were driven mainly by the thick-type columns. Specifically, thick-type columns showed consistently higher activity to the mid-spectral hues, compared to both 1) end-spectral hues, and to 2) achromatic, luminance-varying control gratings. In fact, neither of the end-spectral hues produced significantly higher responses, compared to control activation by the achromatic luminance-varying gratings, in these thick-type stripes (Fig. 5). Based only on that criterion, thick-type columns were not color-selective (relative to luminance) in response to end-spectral hues. Importantly, this finding is consistent with the conventional assumption that thick-type columns in V2 and V3 are not color-selective (Nasr et al., 2016; Tootell and Nasr, 2017). However, mid-spectral hues *did* produce significantly higher responses in these thick-type columns, relative to the luminance grating. Thus, the conventional generality that thick-type columns are not 'color-selective' needs to be qualified: it depends on the hues tested.

These findings also support the conclusion (from a previous MVPA analysis) that voxels within visual areas V1-V3 contain many color-selective neurons, each tuned to a different hue (Brouwer and Heeger, 2009). However here, we extended those findings by showing that, within areas V2 and V3, there are (at least) two different groups of neural clusters with different hue-selectivity tuning curves (Figs. 5 and 7). Consideration of this heterogeneity may improve the accuracy of results based on MVPA.

4.3. Mid-spectral hue preference within thick-type columns

Thick-type columns are generally considered as responsive to achromatic (luminance-varying) stimuli, including responses for orientation and other types of detailed shape encoding. Yoshioka et al. (1996) suggested further that neurons within macaque V2 thick-type stripes also respond to mid-spectral (but not end-spectral) hues (Yoshioka and Dow, 1996; Yoshioka et al., 1996). Consistent with these studies, we found that thick-type columns within human V2/V3 respond selectively to mid-spectral (but not end-spectral) hues, relative to luminance-varying stimuli. Presumably, this lack of end-spectral hue selectivity reduces the deleterious effects of chromatic aberration on fine shape encoding, which would otherwise 'blurs' object resolution within thick-type columns.

4.4. Hue maps within color-selective regions

Electrophysiological and optical studies in macaque have reported that preferred hue within the V2 thin-type stripes (Xiao et al., 2003; Lim et al., 2009) and V4 color-selective patches (Tanigawa et al., 2010) mirrors the spectral continuum, as reflected in the dominant wavelength of the different tested hues. Thus, it can be asked whether those previously reported hue maps in macaque are related to the hue organization that we found here in humans, based on fMRI.

Strictly, these two models may not be mutually exclusive. For one thing, that spectral organization is very small; the spatial scale of the macaque hue maps (roughly 0.5 mm, full cycle, peak to peak) might not be resolved with the fMRI techniques used here (voxel size = 1 mm isotropic). That data was based on optical recordings, which have a much higher spatial resolution compared to fMRI. Although columns in humans are typically ~ twice as large (1-D measurements across the map) as analogous column types in macaques (Tootell and Taylor, 1995; Orban et al., 2004), that correction in expectations would reduce (but not eliminate) the resolution problem in our fMRI, relative to the finer-scale data based on optical recording. Eventually, it may be feasible to test for such continuous (spectrally organized) hue maps in human V2 (and V3), based on higher resolution fMRI techniques.

4.5. Cortical streams

Our data raise the possibility that different combinations of photoreceptors may contribute differentially to correspondingly segregated cortical streams. For instance, given the cone contrasts of our stimuli (Table S1), it might seem likely that M and L cone types (peaking approximately at 530 and 560 nm respectively) (Smith and Pokorny, 1975; Bowmaker and Dartnall, 1980; Schnapf et al., 1987) would contribute strongly to the mid-spectral biases we found in cortex. However, the relationship between cone contrast sensitivity (Cole et al., 1993; Sankeralli and Mullen, 1996) and sensitivity to different hues is complex.

For similar reasons, the S cone (peaking near 420 nm, disregarding pre-retinal filtering) (Smith and Pokorny, 1975; Bowmaker and Dartnall, 1980; Schnapf et al., 1987) may contribute relatively more to the end-spectral responses that we found, at least to the blue (and perhaps also to the red) hues we used. For instance in V1, our observed bias for blue might be construed as supporting the following evidence: 1) many K-cells (in primate LGN) receive strong on-responses from the short-wave (S) cone photopigments (Hendry and Calkins, 1998), and 2) K-cells project to the color-selective V1 blobs (Hendry and Reid, 2000). More generally, the input from S-cones may be enhanced in V1, relative to that in LGN ((De Valois et al., 2000; Solomon and Lennie, 2005) but see (Johnson et al., 2004)).

However, this idea does not explain how the strong bias for end-spectral hues in V1 is inverted in some measurements in V2 and V3. One possible explanation is that thin-type columns show less mid-spectral bias compared to thick-type columns – i.e. a relatively higher responses to end-spectral hues in V2 thin-type (color-selective) columns. However this moderating effect is quite small, relative to the very strong bias for end-spectral hues in V1.

Another possibility is that V1 neurons also respond to mid-spectral hue across a range of luminance levels, but not at isoluminance, as tested here. Such decreases in neuronal response to isoluminant hue variations have been documented previously in V1 and V2 (Gouras and Kruger, 1979; Thorell et al., 1984) and a more recent study reported that such responses were preferentially to mid-spectral hues (Yoshioka et al., 1996). By this idea, the interaction between hue and luminance would decrease from V1 to subsequent visual areas, leading to a stronger response to mid-spectral hues in the higher level areas.

4.6. Occipital temporal color-selective area

In the occipital temporal color-selective area, the fMRI-based hue preference function was a relatively flat line in Fig. 5. Thus, perhaps specific aspects of color perception (measured behaviorally) reflect activity at that relatively higher stage, rather than the spectrally biased activity at lower cortical areas. Consistent with this hypothesis, a direct relationship has been reported between color naming and the cortical representation of color space (based on MVPA at conventional spatial resolution), within this anterior occipitotemporal color-selective site, but not within earlier visual areas (Brouwer and Heeger, 2013). Mullen et al. (2007) also found relatively equal responses to different hue pairs in this occipital temporal area, although they did not test hue relationships *per se*.

4.7. Retinal eccentricity

Prior measurements of color vision have often been restricted to the foveal region of the retina, i.e. within the central 1° of the visual field. Here we instead measured hue responses in the surrounding parafoveal region, from 3 – 10° in the visual field (see Methods). We focused on the parafoveal region for several reasons: 1) to reduce/eliminate possible fMRI contributions from the foveal fixation point and the foveal task, which we used to reduce the extent of eye movement, and to confirm that subjects were continuously attending to the stimulus, and 2) to reduce possible complications due to the yellowing of the macula lutea (Home, 1798; Whitehead et al., 2006), and the absence of short wave ('blue') cones in the central 7–8 min of the retina (Wald, 1967; Bumsted and Hendrickson, 1999).

It is well-known that color vision differs at different eccentricities,

partly reflecting the variation in cone photopigment across eccentricity (Mullen, 1985; Livingstone and Hubel, 1987; Bilodeau and Faubert, 1997; Nasr et al., 2016). To the extent that results here differ from previous studies sampled only within the fovea, it is possible that such hypothetical differences arise from sampling at different eccentricities between studies.

4.8. Relationship of current results to prior studies

As described above, earlier studies of color sensitivity using fMRI in primates (human and non-human) were designed to resolve different (and important) experimental questions, compared to topics of interest here. For instance, several studies focused on the localization of color-selective sites (Zeki et al., 1991; Hadjikhani et al., 1998; Beauchamp et al., 1999; Bartels and Zeki, 2000; Lafer-Sousa et al., 2016; Nasr et al., 2016), relative to luminance-driven activity. Other studies tested cone-selective activation (Engel et al., 1997; Liu and Wandell, 2005; Mullen et al., 2007).

Importantly, the activity produced in these studies was typically produced by a combination of two or more hues. Thus those data do not reveal results that can be directly compared with those here. For instance, extrapolating from our data, the averaged activity produced by a blue-yellow grating and a red-green grating (i.e. each pair of one mid-plus one end-spectral hue) should produce activity levels very similar to each other in V1 – although the reversed pairing (i.e. red-blue (paired end-spectral) or green-yellow(mid-spectral hues)) produces striking differences in activity. Additional stimulus differences between our stimuli and prior stimuli (e.g. cone contrast, spatial and temporal frequency, hue saturation and dominant wavelength) could also contribute. Further studies are required to directly test these possibilities.

Acknowledgements

We thank Professors Marge Livingstone, Patrick Cavanagh and Rhea Eskew for helpful suggestions. This study was supported by NIH grant RO1EY026881 to R.B.H.T. and Massachusetts General Hospital Executive Committee on Research (ECOR) fund Grant 2015A051305 to S.N. and R.B.H.T. Crucial support was also provided by the Martinos Center for Biomedical Imaging and NIH grant 5P41-EB-015896-17, and by the help and cooperation of all of our subjects.

Appendix A. Supplementary data

Supplementary data related to this article can be found at https://doi.org/10.1016/j.neuroimage.2018.07.053.

References

Anderson, S.J., Mullen, K.T., Hess, R.F., 1991. Human peripheral spatial resolution for achromatic and chromatic stimuli: limits imposed by optical and retinal factors. J. Physiol. 442, 47–64.
Bartels, A., Zeki, S., 2000. The architecture of the colour centre in the human visual brain: new results and a review. Eur. J. Neurosci. 12, 172–193.
Beauchamp, M.S., Haxby, J.V., Jennings, J.E., DeYoe, E.A., 1999. An fMRI version of the Farnsworth–Munsell 100-Hue test reveals multiple color-selective areas in human ventral occipitotemporal cortex. Cerebr. Cortex 9, 257–263.
Bilodeau, L., Faubert, J., 1997. Isoluminance and chromatic motion perception throughout the visual field. Vis. Res. 37, 2073–2081.
Bone, R.A., Landrum, J.T., 2004. Heterochromatic flicker photometry. Arch. Biochem. Biophys. 430, 137–142.
Bowmaker, J.K., Dartnall, H., 1980. Visual pigments of rods and cones in a human retina. J. Physiol. 298, 501–511.
Brainard, D.H., 1997. The psychophysics toolbox. Spatial Vis. 10, 433–436.
Breitmeyer, B.G., Tripathy, S.P., Brown, J.M., 2018. Can contrast-response functions indicate visual processing levels? Vision 2, 14.
Brewer, A.A., Liu, J., Wade, A.R., Wandell, B.A., 2005. Visual field maps and stimulus selectivity in human ventral occipital cortex. Nat. Neurosci. 8, 1102–1109.
Brouwer, G.J., Heeger, D.J., 2009. Decoding and reconstructing color from responses in human visual cortex. J. Neurosci. 29, 13992–14003.
Brouwer, G.J., Heeger, D.J., 2013. Categorical clustering of the neural representation of color. J. Neurosci. 33, 15454–15465.
Bumsted, K., Hendrickson, A., 1999. Distribution and development of short-wavelength cones differ between Macaca monkey and human fovea. J. Comp. Neurol. 403, 502–516.
Chang, L., Bao, P., Tsao, D.Y., 2017. The representation of colored objects in macaque color patches. Nat. Commun. 8, 2064.
Cole, G.R., Hine, T., McIlhagga, W., 1993. Detection mechanisms in L-, M-, and S-cone contrast space. Josa a 10, 38–51.
Creutzfeldt, O., Weber, H., Tanaka, M., Lee, B., 1987. Neuronal representation of spectral and spatial stimulus aspects in foveal and parafoveal area 17 of the awake monkey. Exp. Brain Res. 68, 541–564.
Dale, A.M., Fischl, B., Sereno, M.I., 1999. Cortical surface-based analysis. I. Segmentation and surface reconstruction. Neuroimage 9, 179–194.
De Valois, R.L., Cottaris, N.P., Elfar, S.D., Mahon, L.E., Wilson, J.A., 2000. Some transformations of color information from lateral geniculate nucleus to striate cortex. Proc. Natl. Acad. Sci. Unit. States Am. 97, 4997–5002.
Dobkins, K.R., Thiele, A., Albright, T.D., 2000. Comparison of red–green equiluminance points in humans and macaques: evidence for different L: M cone ratios between species. JOSA A 17, 545–556.
Dow, B.M., 2002. Orientation and color columns in monkey visual cortex. Cerebr. Cortex 12, 1005–1015.
Dumoulin, S.O., Harvey, B.M., Fracasso, A., Zuiderbaan, W., Luijten, P.R., Wandell, B.A., Petridou, N., 2017. In vivo evidence of functional and anatomical stripe-based subdivisions in human V2 and V3. Sci. Rep. 7.
Engel, S., Zhang, X., Wandell, B., 1997. Colour tuning in human visual cortex measured with functional magnetic resonance imaging. Nature 388, 68.
Enzmann, D.R., Pelc, N.J., 1992. Brain motion: measurement with phase-contrast MR imaging. Radiology 185, 653–660.
Epstein, R., Kanwisher, N., 1998. A cortical representation of the local visual environment. Nature 392, 598–601.
Felleman, D.J., Lim, H., Xiao, Y., Wang, Y., Eriksson, A., Parajuli, A., 2015. The representation of orientation in macaque V2: four stripes not three. Cerebr. Cortex 25, 2354–2369.
Fischl, B., 2012. FreeSurfer. Neuroimage 62, 774–781.
Fischl, B., Salat, D.H., Busa, E., Albert, M., Dieterich, M., Haselgrove, C., van der Kouwe, A., Killiany, R., Kennedy, D., Klaveness, S., Montillo, A., Makris, N., Rosen, B., Dale, A.M., 2002. Whole brain segmentation: automated labeling of neuroanatomical structures in the human brain. Neuron 33, 341–355.
Fischl, B., Sereno, M.I., Dale, A.M., 1999. Cortical surface-based analysis. II: inflation, flattening, and a surface-based coordinate system. Neuroimage 9, 195–207.
Friston, K.J., Holmes, A.P., Price, C.J., Buchel, C., Worsley, K.J., 1999. Multisubject fMRI studies and conjunction analyses. Neuroimage 10, 385–396.
Geldard, F., 1972. The Human Senses. Wiley, New York.
Gouras, P., Kruger, J., 1979. Responses of cells in foveal visual cortex of the monkey to pure color contrast. J. Neurophysiol. 42, 850–860.
Granger, E.M., Heurtley, J.C., 1973. Letters to the editor: visual chromaticity-modulation transfer function. J. Opt. Soc. Am. 63, 1173–1174.
Greve, D.N., Fischl, B., 2009. Accurate and robust brain image alignment using boundary-based registration. Neuroimage 48, 63–72.
Hadjikhani, N., Liu, A.K., Dale, A.M., Cavanagh, P., Tootell, R.B., 1998. Retinotopy and color sensitivity in human visual cortical area V8. Nat. Neurosci. 1, 235–241.
Hall, S.D., Holliday, I.E., Hillebrand, A., Furlong, P.L., Singh, K.D., Barnes, G.R., 2005. Distinct contrast response functions in striate and extra-striate regions of visual cortex revealed with magnetoencephalography (MEG). Clin. Neurophysiol. 116, 1716–1722.
Hartridge, H., 1947. The visual perception of fine detail. Philos. Trans. R. Soc. Lond. Ser. B Biol. Sci. 519–671.
Hendry, S.H., Calkins, D.J., 1998. Neuronal chemistry and functional organization in the primate visual system. Trends Neurosci. 21, 344–349.
Hendry, S.H., Reid, R.C., 2000. The koniocellular pathway in primate vision. Annu. Rev. Neurosci. 23, 127–153.
Home, E., 1798. XII. An account of the orifice in the retina of the human eye, discovered by professor Soemmering. To which are added, proofs of this appearance being extended to the eyes of other animals. Phil. Trans. Roy. Soc. Lond. 88, 332–345.
Hubel, D.H., Livingstone, M.S., 1987. Segregation of form, color, and stereopsis in primate area 18. J. Neurosci. 7, 3378–3415.
Ives, F.E., 1907. A new color meter. J. Franklin Inst. 164, 47–56.
Johnson, E.N., Hawken, M.J., Shapley, R., 2004. Cone inputs in macaque primary visual cortex. J. Neurophysiol. 91, 2501–2514.
Judd, D., Wyszecki, G., 1975. Physics and psychophysics of colorant layers. In: Color in Business, Science and Industry.
Julesz, B., 1971. Foundations of Cyclopean Perception. University of Chicago Press, Chicago.
Kanwisher, N., McDermott, J., Chun, M.M., 1997. The fusiform face area: a module in human extrastriate cortex specialized for face perception. J. Neurosci. 17, 4302–4311.
Kaskan, P.M., Lu, H.D., Dillenburger, B.C., Kaas, J.H., Roe, A.W., 2009. The organization of orientation-selective, luminance-change and binocular- preference domains in the second (V2) and third (V3) visual areas of New World owl monkeys as revealed by intrinsic signal optical imaging. Cerebr. Cortex 19, 1394–1407.
Keil, B., Triantafyllou, C., Hamm, M., Wald, L.L., 2010. Design optimization of a 32-channel head coil at 7T. In: Proceedings of the 18th Annual Meeting of ISMRM. Stockholm, Sweden 1493.
Lafer-Sousa, R., Conway, B.R., Kanwisher, N.G., 2016. Color-biased regions of the ventral visual pathway lie between face-and place-selective regions in humans, as in macaques. J. Neurosci. 36, 1682–1697.

Landisman, C.E., Ts'o, D.Y., 2002a. Color processing in macaque striate cortex: electrophysiological properties. J. Neurophysiol. 87, 3138–3151.
Landisman, C.E., Ts'o, D.Y., 2002b. Color processing in macaque striate cortex: relationships to ocular dominance, cytochrome oxidase, and orientation. J. Neurophysiol. 87, 3126–3137.
Lim, H., Wang, Y., Xiao, Y., Hu, M., Felleman, D.J., 2009. Organization of hue selectivity in macaque V2 thin stripes. J. Neurophysiol. 102, 2603–2615.
Liu, J., Wandell, B.A., 2005. Specializations for chromatic and temporal signals in human visual cortex. J. Neurosci. 25, 3459–3468.
Livingstone, M.S., Hubel, D.H., 1984. Anatomy and physiology of a color system in the primate visual cortex. J. Neurosci. 4, 309–356.
Livingstone, M.S., Hubel, D.H., 1987. Psychophysical evidence for separate channels for the perception of form, color, movement, and depth. J. Neurosci. 7, 3416–3468.
Lu, H.D., Roe, A.W., 2008. Functional organization of color domains in V1 and V2 of macaque monkey revealed by optical imaging. Cerebr. Cortex 18, 516–533.
Mullen, K.T., 1985. The contrast sensitivity of human colour vision to red-green and blue-yellow chromatic gratings. J. Physiol. 359, 381–400.
Mullen, K.T., Dumoulin, S.O., McMahon, K.L., De Zubicaray, G.I., Hess, R.F., 2007. Selectivity of human retinotopic visual cortex to S-cone-opponent, L/M-cone-opponent and achromatic stimulation. Eur. J. Neurosci. 25, 491–502.
Nasr, S., Liu, N., Devaney, K.J., Yue, X., Rajimehr, R., Ungerleider, L.G., Tootell, R.B., 2011. Scene-selective cortical regions in human and nonhuman primates. J. Neurosci. 31, 13771–13785.
Nasr, S., Polimeni, J.R., Tootell, R.B., 2016. Interdigitated color- and disparity-selective columns within human visual cortical areas V2 and V3. J. Neurosci. 36, 1841–1857.
Nasr, S., Tootell, R.B., 2016. Visual field biases for near and far stimuli in disparity selective columns in human visual cortex. Neuroimage.
Olman, C.A., Van de Moortele, P.F., Schumacher, J.F., Guy, J.R., Ugurbil, K., Yacoub, E., 2010. Retinotopic mapping with spin echo BOLD at 7T. Magn. Reson. Imag. 28, 1258–1269.
Orban, G.A., Van Essen, D., Vanduffel, W., 2004. Comparative mapping of higher visual areas in monkeys and humans. Trends Cognit. Sci. 8, 315–324.
Pelli, D.G., 1997. The VideoToolbox software for visual psychophysics: transforming numbers into movies. Spatial Vis. 10, 437–442.
Peterhans, E., von der Heydt, R., 1993. Functional organization of area V2 in the alert macaque. Eur. J. Neurosci. 5, 509–524.
Polimeni, J.R., Bhat, H., Witzel, T., Benner, T., Feiweier, T., Inati, S.J., Renvall, V., Heberlein, K., Wald, L.L., 2015. Reducing sensitivity losses due to respiration and motion in accelerated echo planar imaging by reordering the autocalibration data acquisition. Magn. Reson. Med.
Polimeni, J.R., Fischl, B., Greve, D.N., Wald, L.L., 2010. Laminar analysis of 7T BOLD using an imposed spatial activation pattern in human V1. Neuroimage 52, 1334–1346.
Poncelet, B.P., Wedeen, V.J., Weisskoff, R.M., Cohen, M.S., 1992. Brain parenchyma motion: measurement with cine echo-planar MR imaging. Radiology 185, 645–651.
Roe, A.W., Ts'o, D.Y., 1999. Specificity of color connectivity between primate V1 and V2. J. Neurophysiol. 82, 2719–2730.
Salzmann, M.F.V., Bartels, A., Logothetis, N.K., Schüz, A., 2012. Color blobs in cortical areas V1 and V2 of the new world monkey Callithrix jacchus, revealed by non-differential optical imaging. J. Neurosci. 32, 7881–7894.
Sankeralli, M.J., Mullen, K.T., 1996. Estimation of the L-, M-, and S-cone weights of the postreceptoral detection mechanisms. JOSA A 13, 906–915.
Schnapf, J., Kraft, T., Baylor, D., 1987. Spectral sensitivity of human cone photoreceptors. Nature 325, 439.
Sereno, M.I., Dale, A.M., Reppas, J.B., Kwong, K.K., Belliveau, J.W., Brady, T.J., Rosen, B.R., Tootell, R.B., 1995. Borders of multiple visual areas in humans revealed by functional magnetic resonance imaging. Science 268, 889–893.
Smith, V.C., Pokorny, J., 1975. Spectral sensitivity of the foveal cone photopigments between 400 and 500 nm. Vis. Res. 15, 161–171.
Solomon, S.G., Lennie, P., 2005. Chromatic gain controls in visual cortical neurons. J. Neurosci. 25, 4779–4792.
Sumner, P., Anderson, E.J., Sylvester, R., Haynes, J.-D., Rees, G., 2008. Combined orientation and colour information in human V1 for both L–M and S-cone chromatic axes. Neuroimage 39, 814–824.
Tanigawa, H., Lu, H.D., Roe, A.W., 2010. Functional organization for color and orientation in macaque V4. Nat. Neurosci. 13, 1542.
Thorell, L.G., de Valois, R.L., Albrecht, D.G., 1984. Spatial mapping of monkey VI cells with pure color and luminance stimuli. Vis. Res. 24, 751–769.
Tootell, R.B., Hamilton, S.L., 1989. Functional anatomy of the second visual area (V2) in the macaque. J. Neurosci. 9, 2620–2644.
Tootell, R.B., Mendola, J.D., Hadjikhani, N.K., Ledden, P.J., Liu, A.K., Reppas, J.B., Sereno, M.I., Dale, A.M., 1997. Functional analysis of V3A and related areas in human visual cortex. J. Neurosci. 17, 7060–7078.
Tootell, R.B., Nasr, S., 2017. Columnar segregation of magnocellular and parvocellular streams in human extrastriate cortex. J. Neurosci. 37, 8014–8032.
Tootell, R.B., Nelissen, K., Vanduffel, W., Orban, G.A., 2004. Search for color 'center(s)' in macaque visual cortex. Cerebr. Cortex 14, 353–363.
Tootell, R.B., Silverman, M.S., Hamilton, S.L., De Valois, R.L., Switkes, E., 1988. Functional anatomy of macaque striate cortex. III. Color. J. Neurosci. 8, 1569–1593.
Tootell, R.B., Taylor, J.B., 1995. Anatomical evidence for MT and additional cortical visual areas in humans. Cerebr. Cortex 5, 39–55.
Ts'o, D., Gilbert, C.D., 1988. The organization of chromatic and spatial interactions in the primate striate cortex. J. Neurosci. 8, 1712–1727.
van der Horst, G.J., Bouman, M.A., 1969. Spatiotemporal chromaticity discrimination. J. Opt. Soc. Am. 59, 1482–1488.
Vanduffel, W., Tootell, R.B., Schoups, A.A., Orban, G.A., 2002. The organization of orientation selectivity throughout macaque visual cortex. Cerebr. Cortex 12, 647–662.
Vautin, R., Dow, B., 1985. Color cell groups in foveal striate cortex of the behaving macaque. J. Neurophysiol. 54, 273–292.
Vimal, R.L.P., 2002. Spatial frequency discrimination: a comparison of achromatic and chromatic conditions. Vis. Res. 42, 599–611.
Wade, A., Augath, M., Logothetis, N., Wandell, B., 2008. fMRI measurements of color in macaque and human. J. Vis. 8 (6), 1–19.
Wade, A.R., Brewer, A.A., Rieger, J.W., Wandell, B.A., 2002. Functional measurements of human ventral occipital cortex: retinotopy and colour. Phil. Trans. Biol. Sci. 357, 963–973.
Wald, G., 1967. Blue-blindness in the normal fovea. JOSA 57, 1289–1301.
Walls, G.L., 1943. Factors in human visual resolution. JOSA 33, 487–505.
Webster, M.A., De Valois, K.K., Switkes, E., 1990. Orientation and spatial-frequency discrimination for luminance and chromatic gratings. Josa a 7, 1034–1049.
Whitehead, A.J., Mares, J.A., Danis, R.P., 2006. Macular pigment: a review of current knowledge. Arch. Ophthalmol. 124, 1038–1045.
Xiao, Y., Casti, A., Xiao, J., Kaplan, E., 2007. Hue maps in primate striate cortex. Neuroimage 35, 771–786.
Xiao, Y., Kavanau, C., Bertin, L., Kaplan, E., 2011. The biological basis of a universal constraint on color naming: Cone contrasts and the two-way categorization of colors. PLoS One 6, e24994.
Xiao, Y., Wang, Y., Felleman, D.J., 2003. A spatially organized representation of colour in macaque cortical area V2. Nature 421, 535–539.
Yacoub, E., Harel, N., Ugurbil, K., 2008. High-field fMRI unveils orientation columns in humans. Proc. Natl. Acad. Sci. U. S. A. 105, 10607–10612.
Yacoub, E., Shmuel, A., Logothetis, N., Ugurbil, K., 2007. Robust detection of ocular dominance columns in humans using Hahn Spin Echo BOLD functional MRI at 7 Tesla. Neuroimage 37, 1161–1177.
Yoshioka, T., Dow, B.M., 1996. Color, orientation and cytochrome oxidase reactivity in areas V1, V2 and V4 of macaque monkey visual cortex. Behav. Brain Res. 76, 71–88.
Yoshioka, T., Dow, B.M., Vautin, R.G., 1996. Neuronal mechanisms of color categorization in areas V1, V2 and V4 of macaque monkey visual cortex. Behav. Brain Res. 76, 51–70.
Zeki, S., 1983. Colour coding in the cerebral cortex: the reaction of cells in monkey visual cortex to wavelengths and colours. Neuroscience 9, 741–765.
Zeki, S., Watson, J., Lueck, C., Friston, K.J., Kennard, C., Frackowiak, R., 1991. A direct demonstration of functional specialization in human visual cortex. J. Neurosci. 11, 641–649.
Zeki, S.M., 1973. Colour coding in rhesus monkey prestriate cortex. Brain Res. 53, 422–427.
Zimmermann, J., Goebel, R., De Martino, F., van de Moortele, P.F., Feinberg, D., Adriany, G., Chaimow, D., Shmuel, A., Ugurbil, K., Yacoub, E., 2011. Mapping the organization of axis of motion selective features in human area MT using high-field fMRI. PLoS One 6, e28716.